

# Heat Transfer around a Circular Cylinder in the Laminar zone

A Thesis Submitted in Partial Fulfilment of  
the Requirements for the degree of

“BACHELOR OF TECHNOLOGY IN CHEMICAL ENGINEERING”



By

BYRI AMOGH VARSH

110CH0093

Under the Guidance of  
Prof. Akhilesh Sahu  
Department of Chemical Engineering,  
National Institute of Technology, Rourkela.

May 2015



## CERTIFICATE

This is to certify that the thesis under the title “Heat Transfer around a Circular Cylinder in the Laminar zone” presented by Byri Amogh Varsh (110CH0093), in partial fulfilments for the requirements of the award of Bachelor of Technology Degree in Chemical Engineering at National Institute of Technology, Rourkela has been carried out under my supervision and guidance.

Date-

Place-

Dr. Akhilesh sahu,

Department of Chemical Engineering,

National Institute of Technology,

Rourkela-769008.

## ACKNOWLEDGEMENT

I would like to express my overwhelming gratitude to Dr. Akhilesh Sahu, my 'Project Guide and Thesis Supervisor' for his enormous help and deep encouragement throughout the process starting from the help in my B.Tech Project completion to the Thesis work. He has been a constant guide and support during any sort of problem during the project. He has provided me with tremendous knowledge on the field of "Computational Fluid Dynamics".

I would like to thank my project mates Pritish, Bishmaya and Eugene and all of my friends for a great company to work with. They have always made the work interesting and the project time to be a fun. I would like to thank Trupti Ranjan Behera and Akhilesh Khappre for constant help in ANSYS software and simulations.

I would like to express my heartfelt gratitude to my parents and my family members those who have supported me emotionally and been a constant support for me throughout my life. I would also thank the Almighty for this wonderful life.

Byri Amogh Varsh,  
110CH0093,  
Department of Chemical Engineering,  
NIT Rourkela.

## ABSTRACT

The present research work is based on the domain of Computational Fluid Dynamics (CFD). The entire work is done in the FLUENT component of ANSYS. The study of flow property has been divided into three phases. The first phase was getting familiar with the software ANSYS-FLUENT and learning its application and utility on the problem of a lid-driven square cavity. The work was done for Newtonian ( $n=1$ ) fluid flow for a set of Reynolds numbers ( $100 < Re < 10,000$ ). The flow was incompressible and in Laminar Regime.

The next phase of the work was to study the problem in hand, i.e., flow past a circular cylinder for a square domain in a unsteady state condition to determine the value of drag coefficient. The flow was taken to be incompressible and in the laminar regime. Here the fluid considered was Newtonian fluid ( $n=1$ ). The values of the drag-coefficient obtained were validated from the literature. Then the final task was to observe the heat transfer flow around circular cylinder for a unsteady state condition and a bit more complicated geometry, i.e., an interim between square and circular geometry for a Newtonian fluid. The study was done by varying the Reynolds number ( $60 < Re < 150$ ). The values of drag-coefficient, lift-coefficient versus time were plotted, and Average Nusselt number versus the Prandtl number were plotted in the considered Reynolds number range. The flow pattern in an unsteady laminar incompressible flow was also studied.

Keywords: Newtonian, Drag Coefficient, Lift Coefficient, Reynolds number, Nusselt number, Prandtl number.

# Contents

---

Topics	PageNo
Certificate	2
Acknowledgement	3
Abstract	4

---

Chapter No	Topics	Page No
	Nomenclature of Symbols	6
	Index of Figures and Tables	7
1.	Introduction	8
2.	Literature Review	9
3.	Problem Statement	11
4.	Results and Discussion	14
	4.1 Lid Driven Cavity	15
	4.2 Heat Transfer past a circular cylinder	19
5.	Conclusions	28
6.	Bibliography	29

# Nomenclature

<u>Symbols</u>	<u>Relevance</u>
<b>D</b>	Diameter of the Cylinder (m)
<b>C<sub>D</sub></b>	Drag Coefficient
<b>C<sub>DP</sub></b>	Pressure component of Drag coeff
<b>n</b>	Power Law Index
<b>C<sub>DF</sub></b>	Friction component of Drag coefficient
<b><math>\nabla</math></b>	$\frac{\partial}{\partial x}i + \frac{\partial}{\partial y}j$
<b>C<sub>P</sub></b>	Pressure Coefficient
<b>F<sub>D</sub></b>	Drag Force (N)
<b>F<sub>DF</sub></b>	Frictional Drag Force (N)
<b>F<sub>DP</sub></b>	Pressure Drag Force (N)
<b>H</b>	Height of the domain Geometry (m)
<b><math>\eta</math></b>	Viscosity (kgm <sup>-1</sup> s <sup>-1</sup> )
<b><math>\rho</math></b>	Density (kg m <sup>-3</sup> )
<b><math>\phi</math></b>	Stream Function
<b>f</b>	Body Force
<b>U<sub>x</sub></b>	x-component of Velocity (m s <sup>-1</sup> )
<b>U<sub>y</sub></b>	y-component of Velocity (m s <sup>-1</sup> )
<b><math>\sigma</math></b>	Stress Tensor
<b>D<sub>∞</sub></b>	Length of Domain Geometry (m)
<b>Y</b>	Ordinate of Mesh
<b>k</b>	Power Law Consistency Index
<b>P</b>	Pressure (Pa)
<b>f</b>	Vortex Shedding Frequency (s <sup>-1</sup> )
<b>U<sub>∞</sub></b>	Inlet velocity
<b>T<sub>∞</sub></b>	Inlet temperature
<b>T<sub>w</sub></b>	Wall temperature
<b>Re</b>	Reynolds number
<b>Nu</b>	Nusselt number
<b>Pr</b>	Prandtl number

# Index of Figures and Tables

Figure No.	Figure Name	Page No.
3.1	Schematics of unsteady Flow around a circular cylinder	12
4.1	Schematics of lid driven Flow in a square Cavity	15
4.2	Stream Function for $50 < Re < 400$ in Square Cavity for Newtonian fluid	16
4.3-4.4	Horizontal central line and Vertical central line Velocity for $Re=100$ and $Re=400$ for Newtonian fluid	17
4.5-4.6	Validation of Horizontal central line and Vertical central line Velocity for $Re=100$ & $400$ for Newtonian fluid	18
4.7	Schematics of Heat transfer around a circular cylinder	20
4.8	Variation of drag with respect to time for different Reynolds number	21
4.9	Variation of lift with respect to time for different Reynolds number	22
4.10-4.11	Streamlines and velocity magnitude for different Reynolds number	23
4.12	Isotherms at different Reynolds number	24
4.13	Surface Nusselt number vs. Time plot for different Reynolds number	25
4.14	Avg surface Nusselt number vs. Prandtl number plot for different Reynolds number	26

# 1. INTRODUCTION

---

There is huge research going on over the bluff –body flows since, it has a huge application in energy conservation. To understand this kind of flow, the simplest obstacle which is a circular cylinder is taken. The most important thing that one must keep in mind is that in circular cylinder there are no distinct separation points of contact unlike in square cylinder which have at its corners. During the extensive study of literature, we found that a homogenous work is presented on Newtonian flow but very scare work on Non – Newtonian flow.

We have numerous equations and numerical models at our disposal for simulating the viscous fluid flow, and in which the most common model used is the Power-Law Model. The finite element method (FEM) has been employed in several studies for investigating the fully developed laminar flow of a power-law non-Newtonian fluid in a rectangular duct. However the finite volume (FV) method is employed mostly in visco-elastic fluid flows [1]. There are numerous drawbacks on employing the FV methods, i.e., induction of artificial diffusion by low order interpolation of the convection term of the Navier–Stokes equations. To overcoming these specified effects, interpolation schemes of higher order have been developed. The most popular scheme is the QUICK (Quadratic Upwind Interpolation for Convective Kinematics) scheme, which is accurate upto the 3<sup>rd</sup> order. Thus, it has higher order of accuracy than low order equations.

The occasional vortex shedding in bluff bodies in the presence of uniform flow has been an area of fascination for researchers and scholars like Leonardo Da Vinci. The origin of the flow can be considered as the instabilities and disruptions occurring in the channel of flow and further it depends largely on the Reynolds number of the fluid. To the engineers the integral parameters that interest are not only the stream functions and vector plots but as well as an extensive study on average nusselt number, Surface nusselt number ,drag, lift, isotherms as well as the Strouhal number. Numerous engineering problems needs the investigation of flows of both nature, i.e., Newtonian ( $n=1$ ) and non-Newtonian (Shear-Thinning  $n<1$  and Shear-Thickening  $n>1$ ). The viscous flow by Non-Newtonian fluids and the categories of related constitutive equations they provide, has enormous utility in petroleum, food industry, lubricants and blood flow. The approach of computational fluid dynamics (CFD) for a non-Newtonian problem is usually more complicated than a Newtonian one as the complexity is increased by the Navier-Stokes constitutive equation of diffusion terms.



## 2. LITERATURE REVIEW

---

Owing to its theoretical and numerical importance, the problem of viscous incompressible fluid flow and forced convection heat transfer around a long cylinder of circular cross-section has been an intensive topic of study for a century. The problem which is being considered has also a model for fundamental studies of challenging fluid mechanics problems. It also represents an important class of engineering applications such as tubular and plate-fin type heat exchangers, cooling towers, hot wire anemometer, nuclear reactor fuel rods, cable-stayed and suspension bridges, offshore risers, sensors and probes, etc. Excellent reviews and survey articles and even entire collection of books are available for the fluid flow over long cylinders of circular cross-section [2-6].

The characteristics of the flow around a circular cylinder changes with the change in Reynolds number according to the following regimes: vortex shedding occurs at  $Re = 50$  and wake transition at  $Re = 180$ . Baranyi [7] did computations for the unsteady momentum and heat transfer for a fixed circular cylinder in the laminar flow regime for the Reynolds number range from 50 to 180. The finite difference method (FV) has been applied to solve the Navier-Stokes and Poisson equations. The diameter of the outer boundary of computation is 30 times more than the diameter of the cylinder and O type grid is used. Drag coefficients and lift coefficients and also Strouhal number variations with the Reynolds number are computed and found out that they are in good agreement with the experimental results, even the 3-D wake formation at about  $Re = 160$  were in good agreement. Posdziech and Grundmann [8] performed 2-D numerical simulations of the flow around the cylinder for  $Re = 5$  to 250 by using spectral element method. They have shown that the unsteady drag variation was smaller as compared to the steady case and the lift coefficient strongly increased with the change in Reynolds number.

Nakamura and Igarashi [9] performed experiments to investigate the change in the heat transfer according to different flow regimes i.e. laminar shedding, shear layer and wake-transition regimes for the Reynolds number range 70 – 30000. The Nusselt number at the rear stagnation point increases with Reynolds number in the laminar shedding regime for  $Re < 150$ . Shi et al. [10] experimentally investigated the effect of temperature dependent viscosity and density of air on the fluid flow and heat transfer from a heated cylinder for the range  $10^{-3} \leq Re \leq 170$ . Isaev et al. [11] has used 2-D Navier-Stokes and energy equations to carry out the numerical calculation of the parameters of unsteady state flow and heat transfer under the conditions of laminar transverse flow for a viscous incompressible fluid around a circular cylinder for the fixed Reynolds number 140. The calculation results have implied that a process of cyclic heating of the wake is observed under these conditions, with the formation of a temperature street similar to Karman vortex street. Mahir et al [12] has investigated the unsteady laminar convective heat transfer from isothermal cylinders of tandem arrangement. The analysis is carried out for the Reynolds numbers of 100 and 200 and for centre-to-centre distance ratio of 2, 3, 4, 5, 7 and 10. The mean and local Nusselt numbers for the upstream and downstream cylinders were computed. It is found that the mean Nusselt number of the upstream cylinder

approaches to that of a single isothermal cylinder for the centre-to-centre distance ratio greater than 4 and the mean Nusselt number of the downstream cylinder is about 80% of the upstream cylinder.

Only for Newtonian fluids, Sharma and Eswaran [13-14] have reported new numerical results on Drag and Lift coefficients and Strouhal number for the values of Reynolds number  $Re \leq 160$ . Typically for an unconfined uniform flow (for Newtonian fluids) oriented transverse to the long axis of the cylinder, the flow remains attached to the surface up to about  $Re = 1-2$  beyond which it gets separated and two-symmetric vortices appear in the rear which remain attached to the surface of the obstacle and grow in length along the direction of flow up to about  $Re = 40-45$  [15]. Under these conditions, the flow field near the obstacle is two-dimensional and depends on time. With further increase in the value of the Reynolds number, the wake became asymmetric and the flow transits to the laminar vortex shedding regime which is characterized in terms of alternate shedding of vortices from the upper half and lower half of the cylinder. This resulted in the flow near the cylinder which is periodic in time, but it is still two-dimensional [15]. Naturally, the changes in the detailed kinematics of the flow also manifest at the macroscopic level, because the global parameters like drag coefficient scale differently with Reynolds number in different regimes. All in all, an adequate body of information is thus available on the momentum transfer coefficients for a square cylinder immersed in Newtonian fluids up to about  $Re < 160$  which is almost the limit of the laminar vortex shedding regime [15]. The effects of confinement and of buoyancy on momentum transfer coefficients have also been studied fairly widely [16-17]. The influence of confining walls on momentum transfer characteristics are modulated by the value of the Reynolds number.

### 3. PROBLEM STATEMENT

---

We considered the two-dimensional unsteady flow of an incompressible fluid (with a uniform velocity ( $U_\infty$ ) and temperature ( $T_\infty$ ) at the inlet) across a circular cylinder is considered as shown in Figure 3.1. The surface of the cylinder is maintained at a constant temperature,  $T_w^*$  ( $> T_\infty$ ). The thermo-physical properties of the streaming fluid does not depend upon the temperature and the viscous dissipation effects are also neglected. The temperature difference between the surface of the cylinder and the streaming liquid is assumed to be low so that the variation of the physical properties, notably, density and viscosity, with temperature could be neglected. Since its an unconfined flow we simulate this problem by confining the obstacle in a box of fictitious boundaries .we choose the dimensions of the box such that,the flow pattern and the temperature profile is unaffected .In the above problem the flow and heat transfer phenomena are governed by continuity ,momentum and thermal energy equations .ANSYS 15 is used for making geometry and meshing purpose ,while FLUENT is used for the simulation.

**Continuity equation:**

$$\nabla \cdot \mathbf{u} = 0 \quad (\text{Equation 3.1})$$

**Momentum Equation:**

$$\text{X-momentum} \quad \frac{\partial u}{\partial t} + \frac{\partial(u*u)}{\partial x} + \frac{\partial(u*v)}{\partial y} = -\frac{\partial P}{\partial x} + \frac{1}{Re} \left( \frac{\partial^2 u}{\partial x^2} + \frac{\partial^2 v}{\partial y^2} \right) \quad (\text{Equation 3.21})$$

$$\text{Y-momentum} \quad \frac{\partial v}{\partial t} + \frac{\partial(v*v)}{\partial y} + \frac{\partial(u*v)}{\partial x} = -\frac{\partial P}{\partial y} + \frac{1}{Re} \left( \frac{\partial^2 u}{\partial x^2} + \frac{\partial^2 v}{\partial y^2} \right) \quad (\text{Equation 3.22})$$

**Energy equation:**

$$\frac{\partial T}{\partial t} + \frac{\partial(V_x T)}{\partial x} + \frac{\partial(V_y T)}{\partial y} = \frac{1}{PrRe} \left( \frac{\partial^2 T}{\partial x^2} + \frac{\partial^2 T}{\partial y^2} \right) \quad (\text{Equation 3.3})$$

Where

Pr=Prandtl number

Re=Reynolds number

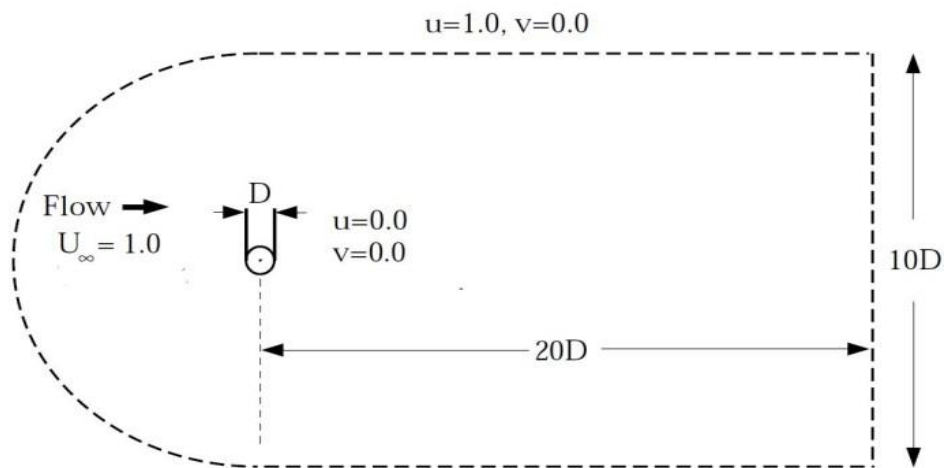


**Fig – (3.1) Schematics of unsteady Flow around a circular cylinder**

Boundary conditions for the problem:-

**At the inlet boundary:** There is a fluid flow of condition

$$U_x = U_\infty \text{ and } U_y = 0. \quad T_\infty = 300\text{K}$$

**On the circular cylinder:** The condition considered is no-slip flow:

$$U_x = 0 \text{ and } U_y = 0. \quad T_w = 310\text{K}$$

**Reynolds number:**

$$\text{Re} = \frac{\rho U_\infty d}{\mu}$$

Where  $\rho$  = Density

$\mu$  = Viscosity

$U_\infty$  = Inlet velocity

$d$  = Diameter

**Prandtl number:**

$$\text{Pr} = \frac{C_p \mu}{k}$$

Where

$C_p$  =specific heat

$k$  =thermal conductivity

$\mu$  =viscosity

**Nusselt number:**

$$\text{Nu} = \frac{hd}{k}$$

Where  $h$ =heat transfer coefficient

$d$ =Diameter

$k$ = thermal conductivity

**Drag and lift coefficients:** The mathematical definition of drag and lift coefficients goes:

$$C_D = \frac{2F_D}{\rho U_\infty^2 D} = C_{DP} + C_{DF}$$

(Here  $F_D$ =Drag Force)

$$C_L = \frac{2F_L}{\rho U_\infty^2 D} \text{ (Here } F_L \text{=Lift Force)}$$

$C_{DP}$  and  $C_{DF}$  are pressure and friction drag coefficients, respectively.

## 4. RESULTS AND DISCUSSION

---

This is the most important part, here all the simulation work is present along with the concept behind it. The content of the part is divided into 2 sub-units:

1. Lid-Driven Square Cavity Problem.
2. Heat transfer in unsteady State flow around a Circular Cylinder Problem.

All of the mentioned topics are covered for Newtonian ( $n=1$ ) type of fluids.

Various Plots and tables are generated in each sub-unit to support the argument presented after this section. Also various Stream Function, and Velocity Magnitude Plot are also presented in order to understand the flow nature in the given domain.

## 4.1 LID DRIVEN SQUARE CAVITY

---

The laminar incompressible flow in a square cavity whose top wall moves with a uniform velocity in its own plane has served over and over again as a model problem for testing and evaluating numerical techniques, in spite of the singularities at two of its corners. For moderately high values of the Reynolds number  $Re$ , published results are available for this flow problem from a number of sources [18-20], using a variety of solution procedures, including an attempt to extract analytically the corner singularities from the dependent variables of the problem [21]. Some results are also available for high Reynolds No [22], but the accuracy of most of these high- $Re$  solutions has generally been viewed with some scepticism because of the size of the computational mesh employed and the difficulties experienced with convergence of conventional iterative numerical methods for these cases. possible exceptions to these may be the results obtained by Benjamin and Denny (41 for  $Re = 10,000$  using a non-uniform  $151 \times 151$  grid such that  $\Delta_x = \Delta_y = 1/400$  near the walls and those of Agarwal [23 ] for  $Re = 7500$  using a uniform  $121 \times 121$  grid together with a higher order accurate upwind scheme.

The present study aims at studying the fluid flow in the lid-driven square cavity for a set of Reynolds Number  $100 < Re < 10,000$  for the Newtonian fluids .The Stream functions at all of the considered Reynolds number are found out. And for the validation purpose Ghia et al. [24] was considered (4.2). Here the y-component of the velocity at horizontal centre line and x-component at vertical centre line is found out (4.5-6).

The geometry is a simple square one with top lid being a moving wall with a velocity that can be evaluated from the expression of Reynolds No given the material under use is water. Here the mesh is normal square mesh of dimension  $151 \times 51$  found from [24]. With a specified residual in continuity and both the momentum transport equation being  $< 10^{-6}$  the converged solution is plotted.

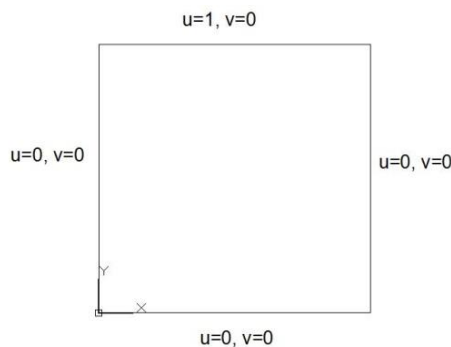
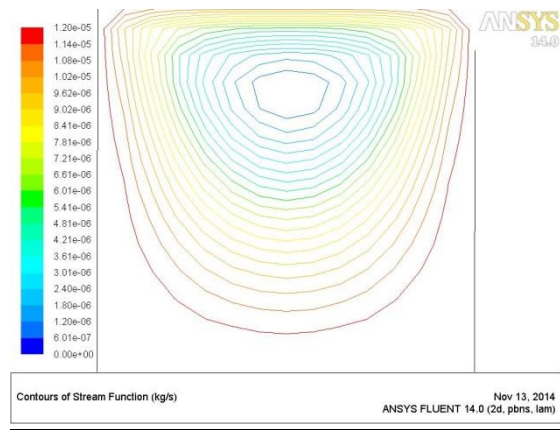


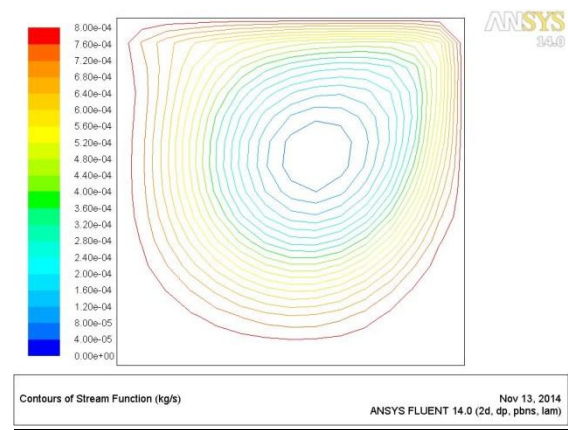
**Fig-4.1 Schematics of lid-driven flow in a square cavity**

## 1. Stream Function Plot for various Reynolds Number for Newtonian fluid:

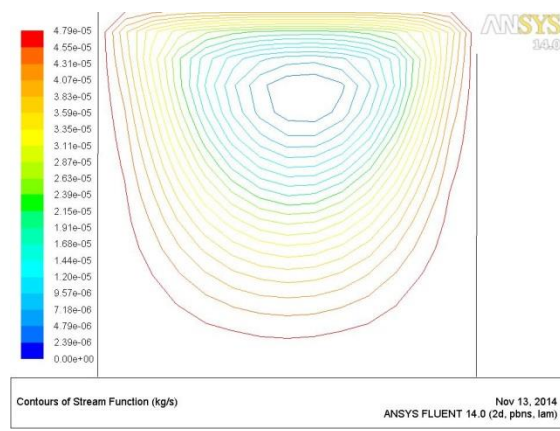
The above below are for the instantaneous Stream lines contours for different values of Reynolds Number are shown. These plots demonstrate the nature of fluid flow in the geometry. The variation is considered from Reynolds no  $100 < Re < 10,000$ .



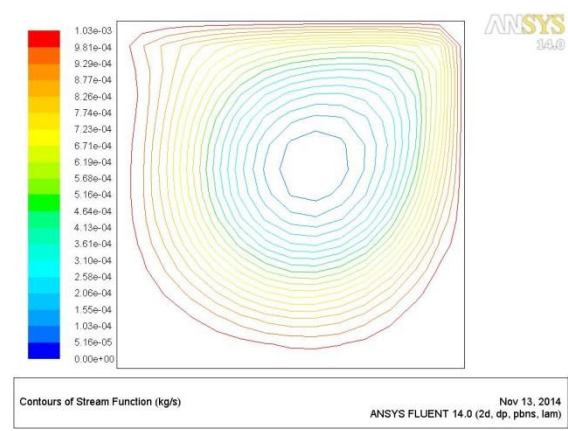
(a)



(b)



(c)



(d)

**Fig 4.2 Streamline patterns for (a) Re=100 (b) Re=20000 (c) Re=400 (d) Re=10000**

At lower value of Reynolds No say at Re=100, the position of wake is somewhat at the centre with respect to the horizontal plane. But, as we have increased the Reynolds No the wake portion is shifted towards the right hand portion of the cavity. This is because at higher Reynolds No the velocity is quite high which affects the wake in the given manner



## 2. Horizontal Centre line and Vertical Centre Line Velocity for various Reynolds No for Newtonian Fluid:

The first two figures demonstrate the vertical component of horizontal centre line and the horizontal component of vertical centre line. The variation is considered for Reynolds No=100 and 400

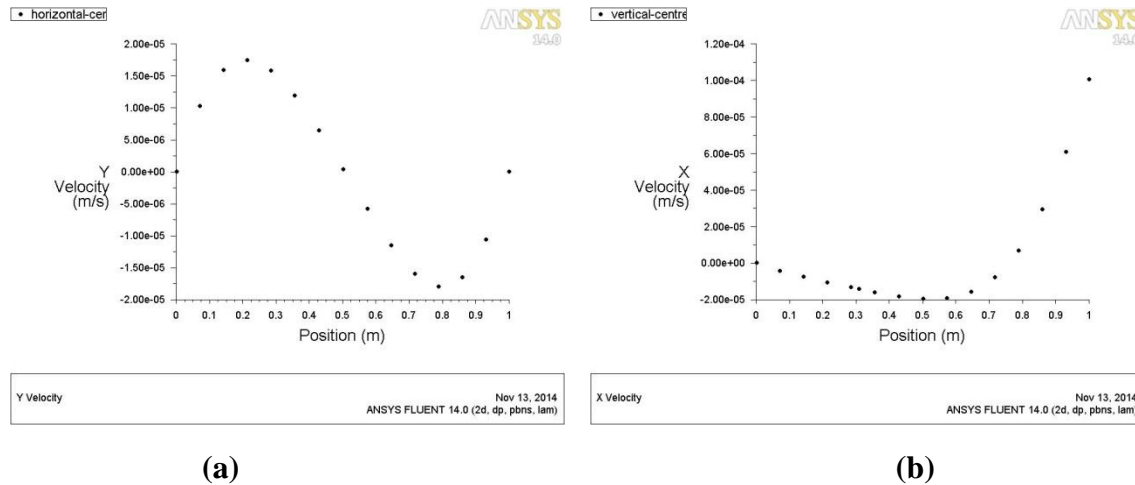


**Fig 4.3 (a) Horizontal centre line velocity and (b) Vertical centre line velocity for  $Re=100$**

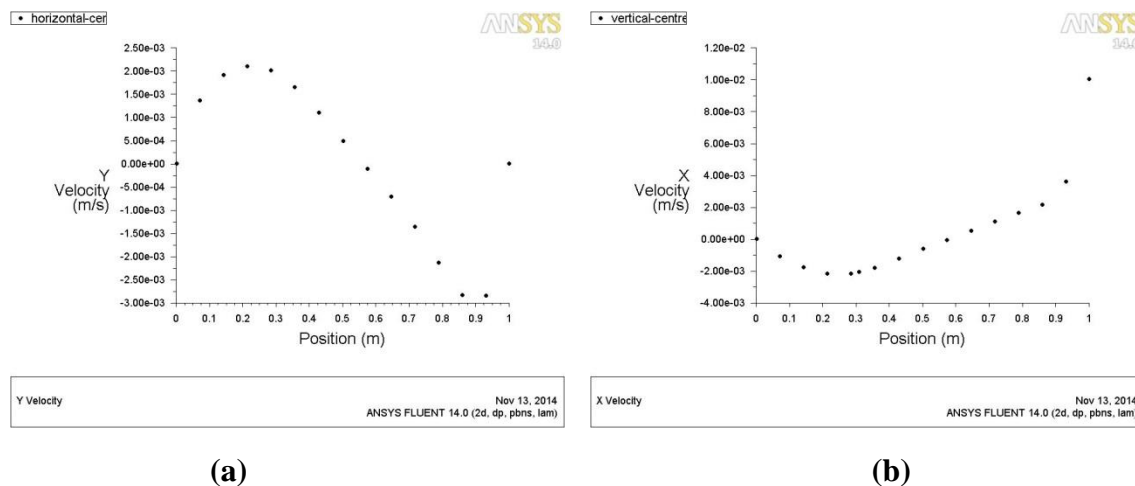
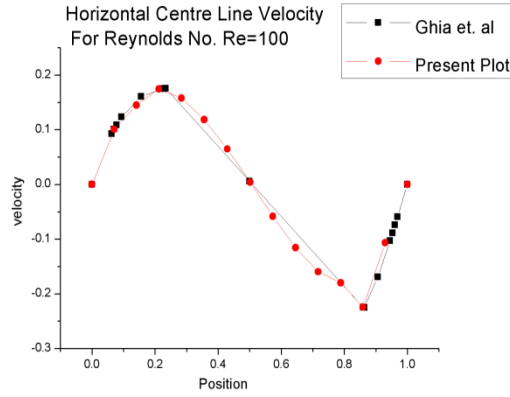


**Fig 4.4 (a) Horizontal centre line velocity and (b) Vertical centre line velocity for  $Re=400$**

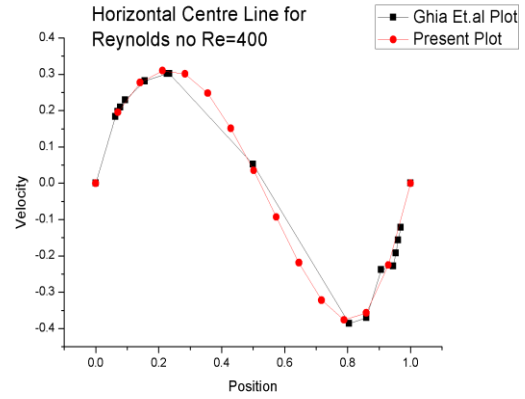
The first half of horizontal central line has the flow in upward direction and as we move from the wall towards the centre the velocity initially is zero due to no slip condition and then the velocity increases to a maximum and further drops to zero due to its distance from the walls and the effects were not felt at the centre and further moving away from the centre in the right half the velocity/ flow direction is downward direction which can be seen in the plot. The bottom portion of vertical central line practically has zero velocity at the walls due to the no slip boundary condition has zero velocity at the proximity of bottom wall. The top wall velocity is fixed the lid velocity which can be seen from the plot

### 3. Validation from literature with plots from Ghia et al. for Newtonian flow:

This section of the discussion is dedicated towards the validation of the results obtained from Ghia et al. Work [25]. The main purpose of validation is to demonstrate the consistency of model.

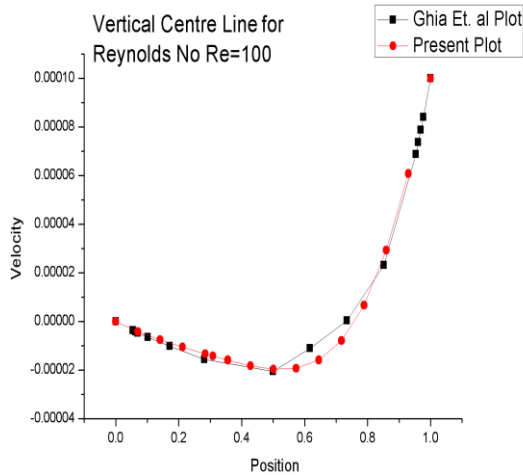


(a)

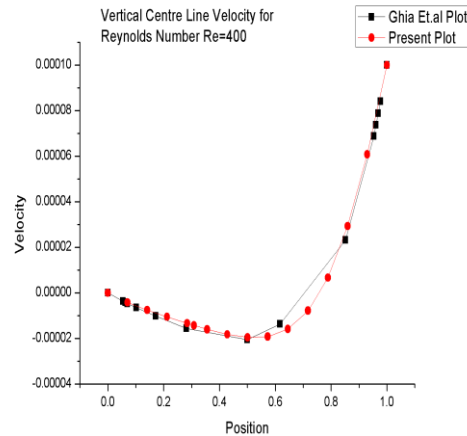


(b)

**Fig 4.5 Horizontal centre line velocity for (a) Re=100 (b) Re=400**



(a)



(b)

**Fig 4.6 Vertical centre line velocity for (a) Re=100 (b) Re=400**

The value obtained for x-component of velocity at vertical centre line and y-component of velocity at horizontal centre line is plotted for Reynolds No 100 and 400 values. These results obtained are quite encouraging. This shows that the setup we used is infact in accordance with that in the literature.

## 4.2 HEAT TRANSFER IN UNSTEADY STATE FLOW PAST A CIRCULAR CYLINDER

---

The present numerical study has been carried out using **FLUENT** (version 15). The unstructured ‘quadrilateral’ cells of non-uniform spacing were generated using **Geometry** and **Meshing** Section of **ANSYS**. The grid near the surface of the cylinder was sufficiently fine to resolve the flow within the boundary layer. For further refining of the grid in was used. Furthermore, the unsteady laminar segregated solver was used with second order upwinding scheme for the convective terms in the momentum equation. The semi-implicit method for the pressure linked equations (**SIMPLE**) scheme was used for pressure–velocity coupling a. In the present study, a convergence criterion of  $1 \times 10^{-10}$  was used for the residuals of all variables. The iterations were stopped when the oscillations of the lift coefficients either reached a periodic steady state or when these die out completely.

Here the geometry used is shown in fig below,i.e input wall is circular in nature. After inputting the upstream and downstream lengths, next comes the turn of meshing. As discussed already, for a circular cylinder a **triangular mesh** is needed [26]. The dimension of mesh is taken to be 251 x 251 [25]. The inlet, top and bottom wall is mentioned as velocity inlet whereas the cylinder is taken to be no slip wall. The outlet is maintained as **Pressure-Outlet** Condition. There exists a symmetric condition at top and bottom wall. It needs to be broken in order to obtain time-dependent Drag. This is done by incorporating custom field function after standard initialisation is done.

Here for Newtonian flow, the velocity is taken to be 1m/s, viscosity of the fluid is varied according to different Prandtl number. For different values of Reynolds No the corresponding density is fixed while keeping others constant. Now for different sets of Reynolds no different values of drag, value of Lift and surface Nusselt no is evaluated. The plots of drag and lift for sets of Reynolds no is shown (4.8-9). The stream function and velocity magnitude are in (4.10-11). Here time step is 0.2 sec with 2000 time steps in total. The final plot of the values of Average Nusselt no vs Prandtl no for differenet Reynolds no were drawn for further study.

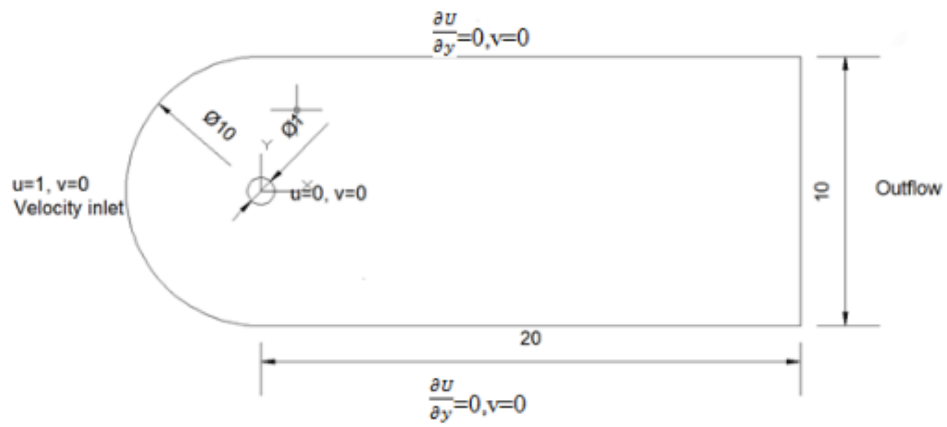


**Fig 4.7 Schematics of Heat transfer around a circular cylinder**

**1. Time dependency of Drag and Lift Coefficient for various Reynolds No for Newtonian flow:**

Here the values of drag coefficients and lift coefficients were plotted for various values of Reynolds no  $60 < Re < 150$  against time. The plots of  $Re=90$ , 100 and 120 are displayed for different Prandtl no.

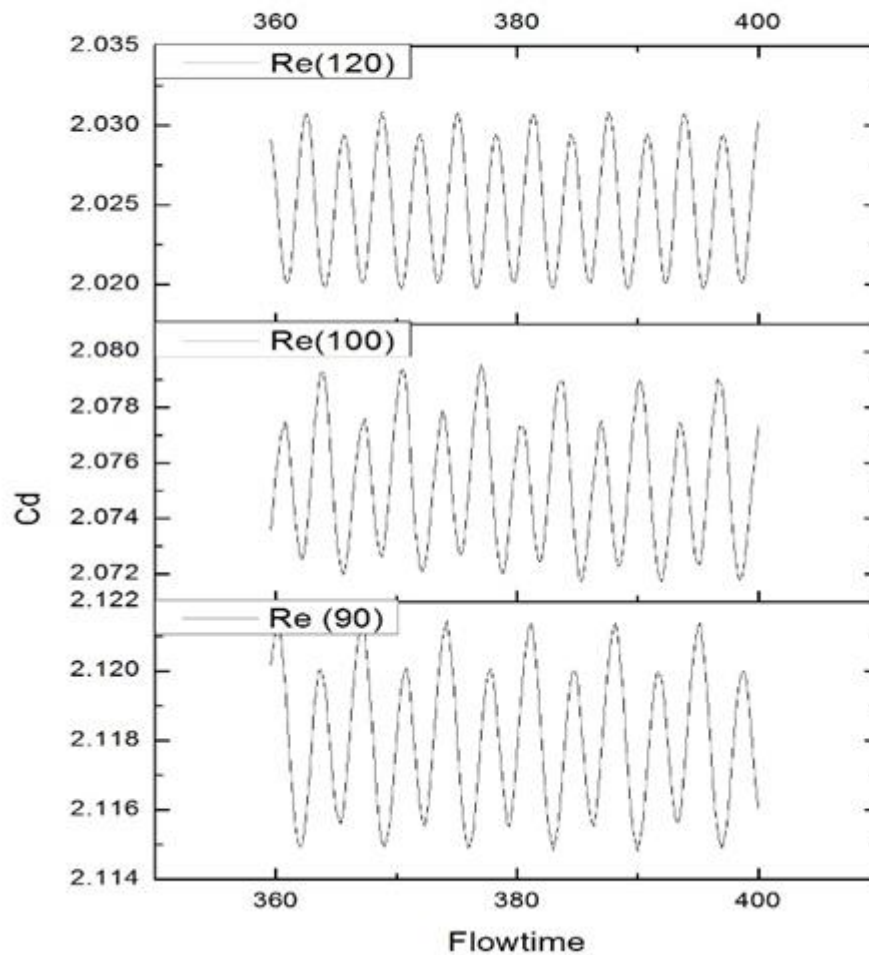


**Fig 4.8 Drag for different Reynolds No at Prandtl No=0.7**

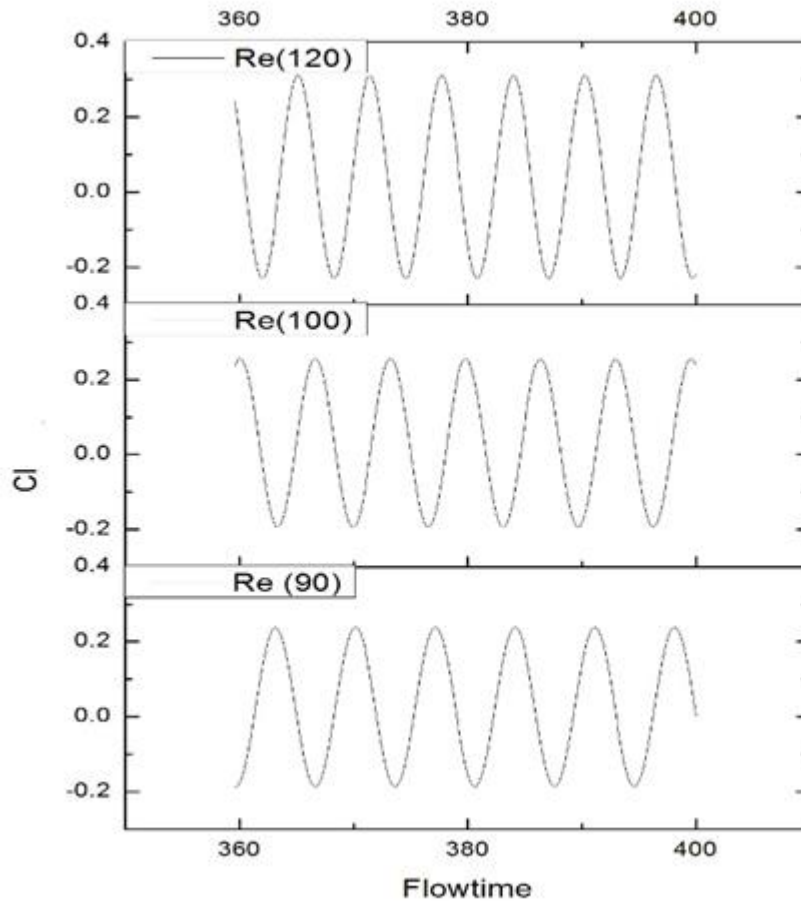


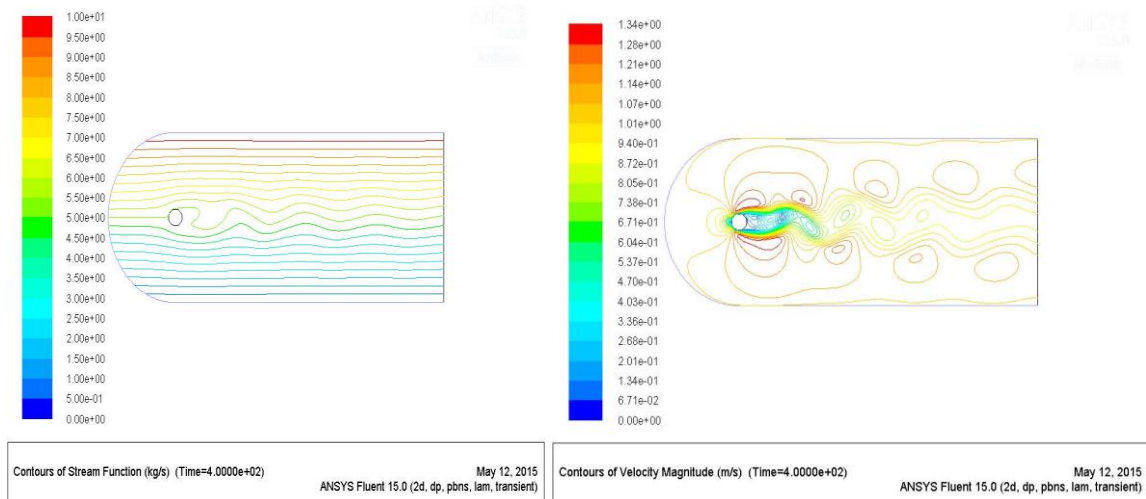
**Fig 4.9 Lift for different Reynolds No at Prandtl No=0.7**

It was found that the drag for Re-90 is remaining constant that is steady state is still remaining for Re-90. It was also observed from the plots of drag and lift with respect to time that time necessary to complete one cycle of lift is more or less the same time necessary to complete two cycles of drag. Thus, the frequency of drag cycle is twice that of the lift cycle. The frequency with which the lift cycle varies is known as the vortex shedding frequency. So, the drag frequency is double the vortex shedding frequency.

The plots of drag and lift coefficients were shown for different Reynolds number at Prandtl number =0.7 (generally  $Pr=0.7$  is for air). From the above plots we observe that, as the Reynolds number increased the curves became more and more smooth

## 2. Instantaneous Streamlines and Velocity Magnitude for various Reynolds No for Newtonian flow:

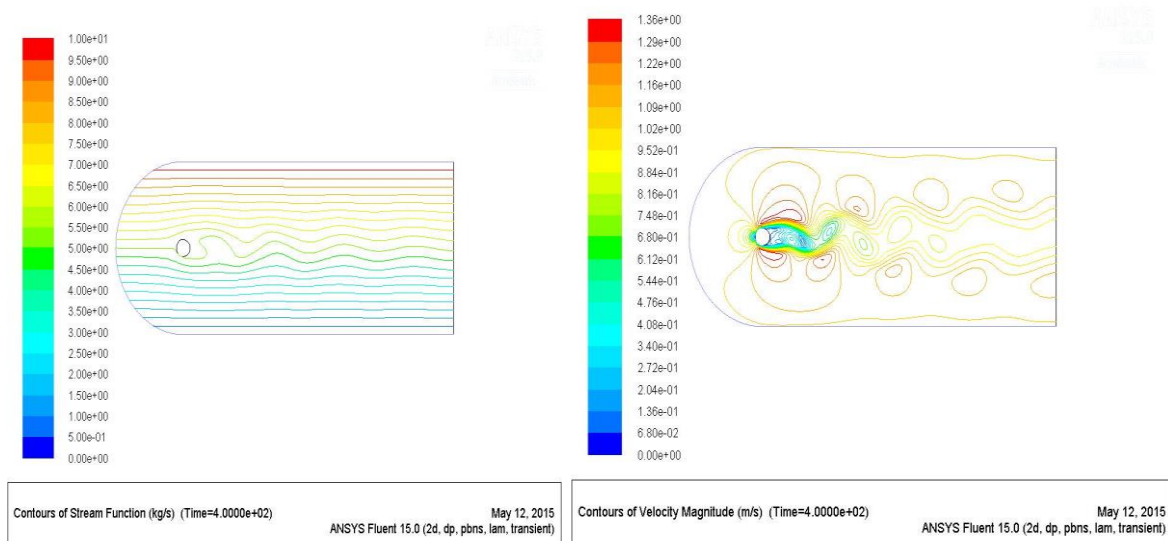
The left plots denote the instantaneous streamlines for increasing Reynolds No and the plots on the right denote the contours of velocity magnitude. Though we have the plots for all the intermediate values but the plots of the extreme values are shown. This is done to cover the entire regime.



(a)

(b)

**Fig 4.10 (a) Streamlines and (b) Velocity magnitude for Reynolds No =100**



(a)

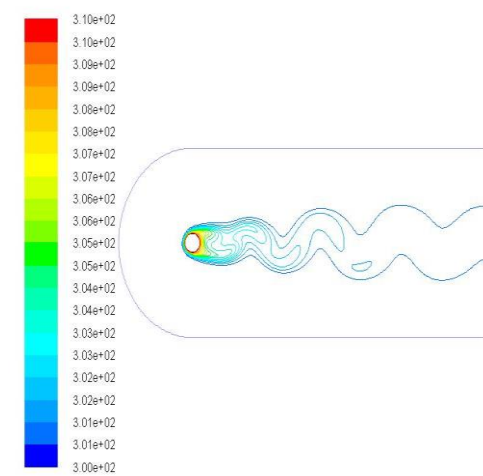
(b)

**Fig 4.11(a) Streamlines and (b) Velocity magnitude for Reynolds No =120**

From the above contours we can observe the flow and the velocity profile of the fluid over the circular cylinder

### 3. Instantaneous Isotherms for various Reynolds No for Newtonian flow:

The plots below show the temperature past the circular cylinder (heat transfer across the circular cylinder). Below are the plots for Reynolds no =100 and for different Prandtl no.

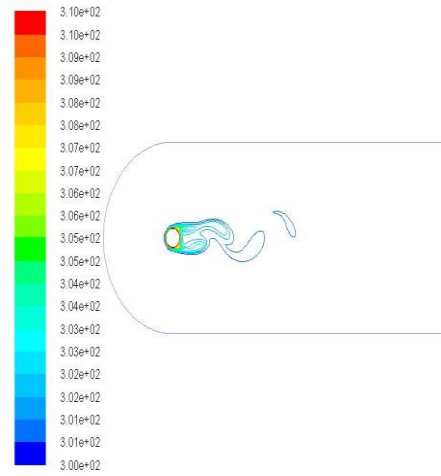


Contours of Static Temperature (K) (Time=4.0000e+02)

ANSYS Fluent 15.0 (2d, dp, pbns, lam, transient)

May 12, 2015

(a)

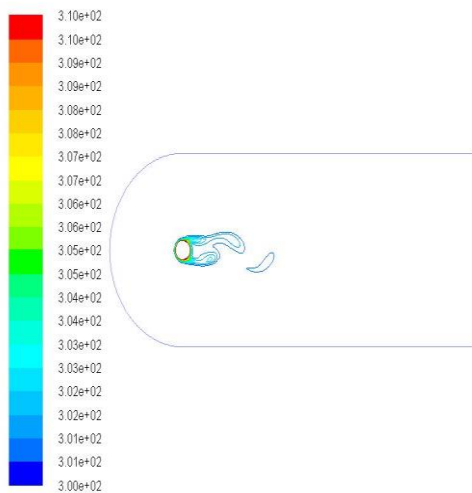


Contours of Static Temperature (K) (Time=4.0000e+02)

ANSYS Fluent 15.0 (2d, dp, pbns, lam, transient)

May 12, 2015

(b)

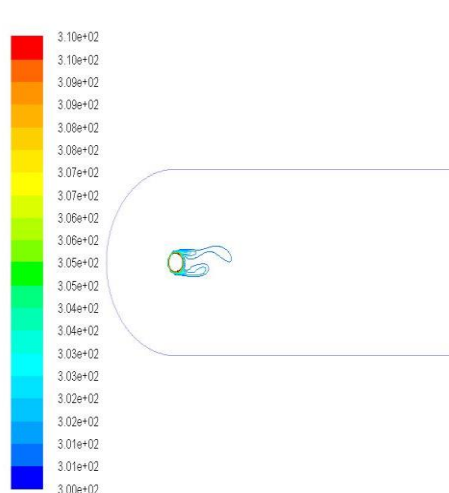


Contours of Static Temperature (K) (Time=4.0000e+02)

ANSYS Fluent 15.0 (2d, dp, pbns, lam, transient)

May 12, 2015

(c)



Contours of Static Temperature (K) (Time=4.0000e+02)

ANSYS Fluent 15.0 (2d, dp, pbns, lam, transient)

May 12, 2015

(d)

**Fig 4.12 Isotherms at Reynolds No =100 for (a) Prandtl No=0.7 (b) Prandtl No=5  
(c) Prandtl No=10 (d) Prandtl No=20**



**4. Time dependency of Surface Nusselt No for different Reynolds No for Newtonian flow:**

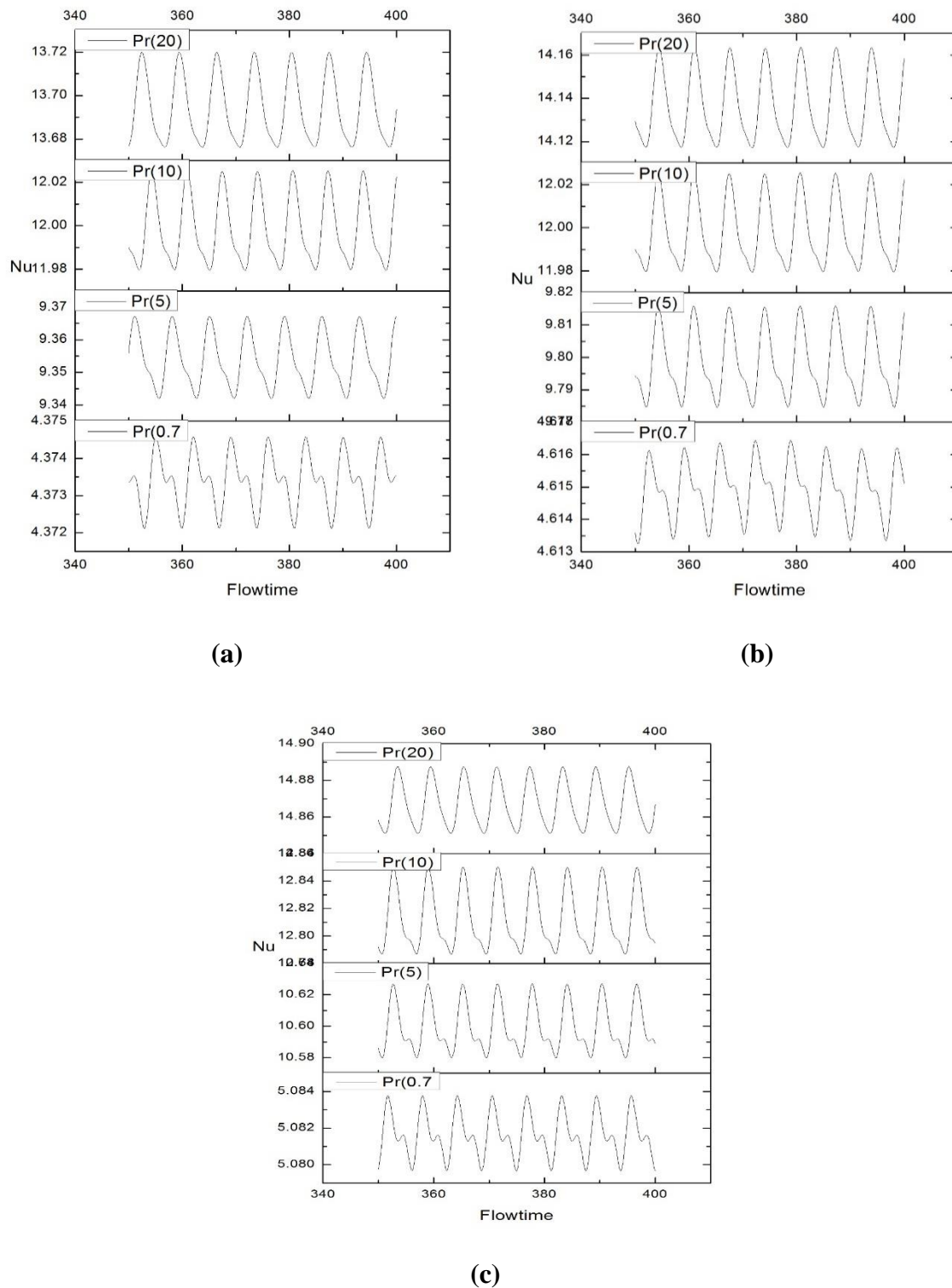


**Fig 4.13 Surface Nusselt No versus Flowtime at (a) Re=90 (b) Re=100 and (c) Re=120**

The above plots denote the Surface Nusselt number at different Prandtl no at varying Reynolds No. The plots obtained for varying Prandtl No and same Reynolds No are merely the same.

## 5. Post Processing of Results

This section is dedicated for the post-processing part. Since we are intrested in heat transfer past a circular cylinder,we calculated then surface Nusselt number which is dependant on time . So, for studying the impact of the surface Nusselt number we need to determine the avg Nusselt number and study how it varies when it's plotted against Prandtl number.

**Table-4.25 (Average Surface Nusselt No v/s Prandtl No at varying Reynolds No)**

<b>Prandtl Number</b>	<b>Avg Nusselt Number(Re=90)</b>	<b>Avg Nusselt Number(Re=100)</b>	<b>Avg Nusselt Number(Re=120)</b>
<b>0.7</b>	<b>4.373422243</b>	<b>4.614946588</b>	<b>5.081600196</b>
<b>5</b>	<b>9.353209643</b>	<b>9.798748657</b>	<b>10.59903663</b>
<b>10</b>	<b>11.864311943</b>	<b>11.99905842</b>	<b>12.81213698</b>
<b>20</b>	<b>13.69364346</b>	<b>14.13716538</b>	<b>14.86685724</b>

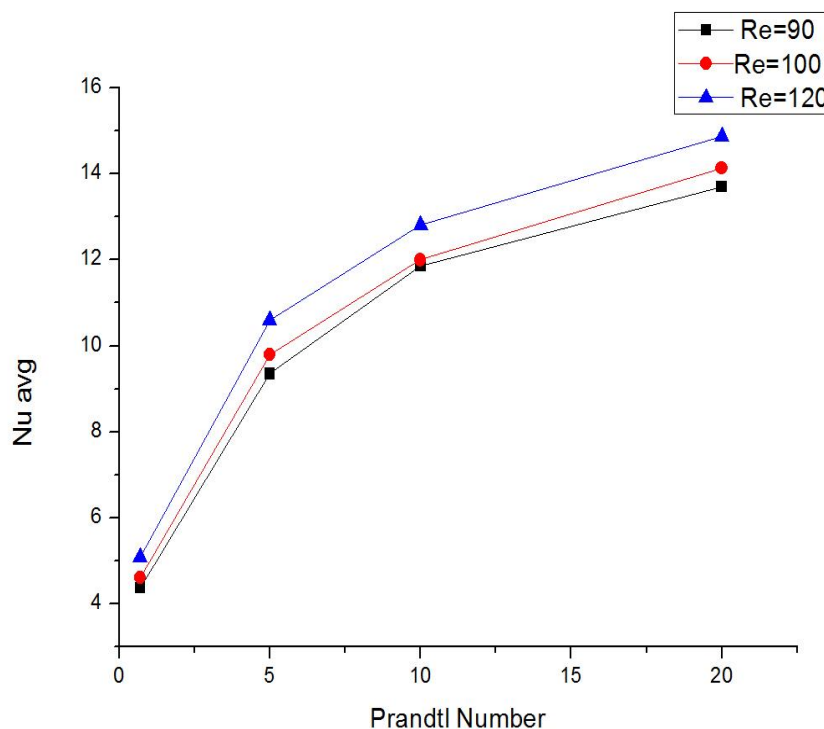


**Fig 4.14 Average surface Nusselt no v/s Prandtl no**

## 5. CONCLUSIONS

---

For the square cavity problem, the results obtained for Newtonian was in well accordance with the ones in literature. This means that the simulation setup was a close approximation of the real time problem.

Now, for heat transfer in an unsteady flow past a circular cylinder, the time dependency of drag coefficients and lift coefficients were visible for  $Re > 70$  for Newtonian fluids. Flow pattern is presented though the instantaneous streamline and velocity magnitude profiles across the circular cylinder. The detailed temperature fields near the obstacle are presented via instantaneous isotherms. The temporal variation of the average Nusselt number is presented. The time averaged Nusselt number increases with the increase in the Reynolds number for the fixed value of the Prandtl number ( $Pr=0.7$ ).

## 6. BIBLIOGRAPHY

---

- [1]. P. Y. Huang, J. Feng.: Wall effects on the flow of viscoelastic fluids around a circular cylinder. *J. Non-Newtonian Fluid Mech.* 60, 179–198 (1995).
- [2]. Ahmad, R.A., 1996, Steady-state numerical solution of the Navier-Stokes and energy equations around a horizontal cylinder at moderate Reynolds numbers from 100 to 500, *Heat Transfer Eng.*, 17: 31–81.
- [3]. Lange, C. F., Durst F., Breuer M., 1998. Momentum and heat transfer from cylinders in laminar cross flow at  $10^{-4} \leq Re \leq 200$ , *Int. J. Heat Mass Transfer*, 41: 3409 - 3430.
- [4]. Norberg, C., 2003. Fluctuating lift on a circular cylinder: review and new measurements, *J. Fluids Structures*, 17: 57 – 96.
- [5]. Zdravkovich, M. M., 1997. *Flow Around Circular Cylinders: Fundamentals*, Oxford University Press, New York, vol. 1.
- [6]. Zdravkovich, M. M., 2003. *Flow Around Circular Cylinders: Fundamentals*, Oxford University Press, New York, vol. 2.
- [7]. Baranyi, L., 2003. Computation of unsteady momentum and heat transfer from a fixed circular cylinder in laminar flow, *J. Computational Applied Mechanics*, 4: 13 – 25.
- [8]. Posdziech, O., Grundmann, R., 2007 A systematic approach to the numerical calculation of fundamental quantities of the two-dimensional flow over a circular cylinder, *J. Fluids Structures*, 23 : 479 – 499 .
- [9]. Nakamura H. and Igarashi T., 2004. Variation of Nusselt number with flow regimes behind a circular cylinder for Reynolds numbers from 70 to 30000, *Int. J. Heat and Mass Transfer*, 47 (23), pp. 5169 –5173.
- [10]. Shi, J.-M., Gerlach, D., Breuer, M., Biswas, G. and Durst F., 2004. Heating effect on steady and unsteady horizontal laminar flow of air past a circular cylinder, *Phys. Fluids* 16, pp. 4331 – 4345.
- [11]. Isaev, S. A., Leontiev, A. I., Kudryavtsev, N. A., Baranova, T. A., Lysenko, D. A., 2005. Numerical simulation of unsteady state heat transfer under conditions of laminar transverse flow past a circular cylinder, *High Temperature*, 43 : 746 – 759.
- [12]. Mahir, N. and Altac, Z., 2008. Numerical investigation of convective heat transfer in unsteady flow past two cylinders in tandem arrangements, *Int. J. Heat Fluid Flow*, 29, pp. 1309–1318.
- [13]. R.P. Chhabra, J.F. Richardson, *Non-Newtonian Flow and Applied Rheology: Engineering Applications*, second ed., Butterworth-Heinemann, Oxford, 2008.
- [14]. R.P. Chhabra, *Bubbles, Drops and Particles in Non-Newtonian Fluids*, second ed., CRC Press, Boca Raton, FL, 2006.
- [15]. P. Sivakumar, R. P. Bharti, R.P. Chhabra, “Effect of power-law index on critical parameters for power-law flow across an unconfined circular cylinder” *Chemical Engineering Science* 61 (2006) 6035 – 6046.
- [16]. W.R. Schowalter, *Mechanics of Non-Newtonian Fluids*, Pergamon, Oxford, UK 1977.
- [17]. R. Clift, J. Grace, M.E. Weber, *Bubbles, Drops and Particles*, Academic, New York, 1978.
- [18]. K. N. Ghia, W. L. Hankey AND J. K. Hodge, “Study of Incompressible Navier-Stokes Equations in Primitive Variables Using Implicit Numerical Technique,” *AIAA Paper No. 77-648*, 1977; *AIAA J.* 17(3)(1979), 298.
- [19]. Polynomial interpolation methods for viscous flow calculations S. G. Rubin, P. K. Khosla, *J. Comput. Phys.* 24(3) (1977) 217.

- [20]. R. E. Smith, A. Kidd, "Comparative Study of Two Numerical Techniques for the Solution of Viscous Flow in a Driven Cavity," pp. 61-82, NASA SP-378, 1975.
- [21]. K. N. Ghia, C. T. Shin, AND U. Ghia, "Use of Spline Approximations for Higher-Order Accurate Solutions of Navier-Stokes Equations in Primitive Variables," AIAA Paper No. 79-1467, 1979.
- [22]. M. Nallaswamy AND K. K. Prasad, J. Fluid Mech. 79(2) (1977), 391.
- [23]. R. K. Agarwal, "A Third-Order-Accurate Upwind Scheme for Navier-Stokes Solutions at High Reynolds Numbers," AIAA Paper No. 81-0112, 1981.
- [24]. U. Ghia, K. N. Ghia AND C. T. Shin, "High-Re Solutions for Incompressible Flow Using the Navier-Stokes Equations and a Multigrid Method" J. comput phs 48, 387-411 (1982).
- [25]. M. Coutanceau, J. R. Defaye, Circular Cylinder Wake Configurations – A Flow Visualization Survey, Appl. Mech. Rev., 44(6), June 1991.